Revisiting MODFLOW's Capability to Model Flow Through Sedimentary Structures

Bardot, Kerry; Lesueur, Martin; Siade, Adam J.; McCallum, James L.

DOI
10.1111/gwat.13273

Publication date
2022

Document Version
Final published version

Published in
Groundwater

Citation (APA)
Bardot, K., Lesueur, M., Siade, A. J., & McCallum, J. L. (2022). Revisiting MODFLOW's Capability to Model Flow Through Sedimentary Structures. *Groundwater*, *61*(5), 663-673. https://doi.org/10.1111/gwat.13273

Important note
To cite this publication, please use the final published version (if applicable).
Please check the document version above.

Groundwater

Revisiting MODFLOW's Capability to Model Flow Through Sedimentary Structures

by Kerry Bardot[1], Martin Lesueur[2,3], Adam J. Siade[2,4], and James L. McCallum[2]

Abstract

Sedimentary structures have unique geometries and anisotropic hydraulic conductivity, both of which control groundwater flow. Traditional finite-difference simulators (e.g., MODFLOW) have not been able to correctly represent irregular, dipping and anisotropic structures due their use of a simplified conductivity tensor, causing many modelers to turn toward finite-element codes with their sophisticated meshing capabilities. However, the release of MODFLOW 6 with its flexible discretization and multipoint flux approximation scheme prompts us to revisit its capability to compute flow through complex sedimentary structures. Through the use of a novel benchmark and case study, we show that when versions previous to MODFLOW 6 are applied to dipping structures, modeled fluxes and hence flow through the system, can be significantly over or underestimated. For example, effective conductivity for a 30° dipping layer with a 100:1 conductivity ratio is reduced to only 2% of its inputted value. We show that MODFLOW 6, with its XT3D capability and flexible discretization options is far superior to its predecessors, allowing flow through complex sedimentary structures to be simulated more accurately. However, on vertically offset grids, which have been available in all versions of MODFLOW and are often used in practice, loss of accuracy is still a concern when the vertical offset is large, that is, the dip of the sedimentary layer is steep, particularly if the layer is much more conductive than the surrounding material. The hypothesis that vertically offset grids lack sufficient hydraulic connectivity between adjacent model layers to accurately simulate the steeply dipping, highly heterogeneous case is a topic for further investigation.

Introduction

Sedimentary basins contain vast amounts of freshwater and need to be carefully managed to secure their longevity. Basins are comprised of discrete sedimentary structures (from herein "structures") of unique shape and orientation following millions of years of deposition, erosion and tectonics. Although basins hosting groundwater resources are predominantly horizontal and extensive, folding and faulting can induce tilting of structures, and erosion can cause units to have irregular lateral boundaries (Catuneanu 2006; Fossen 2016). Furthermore, deposition and consolidation cause sedimentary units to exhibit anisotropic hydraulic conductivity up to 10,000:1 at a regional scale (Michael and Voss 2009; Yager et al. 2009), with maximum conductivity oriented parallel to geologic deposition. Structures of primary interest for water supply are the connected highly permeable sand bodies related to extensive shoreline or dune systems, as well as the connected low permeability structures deposited in low energy settings which can cause compartmentalization of flow systems (Koltermann and Gorelick 1996; Oriani and Renard 2014). Geological models developed for flow modeling in sedimentary basins, where these structures are ubiquitous, must preserve their physical shape and hence connectivity. The flow model must equally ensure that connected and true flow paths are recreated (Renard and Allard 2013). Groundwater models must therefore represent the geometry and principal direction of conductivity associated with sedimentary structures, and solve for the sharp changes in flow direction that these structures generate.

Among numerical groundwater models, MODFLOW is one of the most widely used codes (Harbaugh 2005; Kumar 2019). MODFLOW is open source with a variety of GUIs and an extensive range of plugins to suit various hydrological scenarios. However, MODFLOW

[1]Corresponding author: School of Earth Sciences, University of Western Australia, Perth, Australia; kerry.bardot@research.uwa.edu.au

[2]School of Earth Sciences, University of Western Australia, Perth, Australia

[3]Computational Mechanics, Delft University of Technology, Delft, Netherlands

[4]CSIRO Land and Water, Wembley, Western Australia

Article impact statement: Numerical misrepresentation of structures in groundwater models can cause significant error in modeled flow.

Received June 2022, accepted November 2022.

doi: 10.1111/gwat.13273

has historically been limited to Cartesian discretization and a two-point finite-difference scheme, which is not suitable for geometrically complex hydrogeological units (Hoaglund and Pollard 2003; Li et al. 2010; Gao et al. 2021). The two-point flux approximation (TPFA) in MODFLOW has an inherent orthogonality assumption whereby the conductivity tensor must align with cell boundaries (Harbaugh 2005). Problems arise when structures and their conductivity tensors are nonuniformly tilted in the vertical direction, and when their irregular shape becomes significantly rasterized when mapped onto a structured grid. Accordingly, the modeling of fluid flow in complex sedimentary reservoirs has been undertaken using finite-element (FE) (Yager et al. 2009; Fries et -al. 2014; Borghi et al. 2015) and finite volume (FV) (Rühaak et al. 2008; Panday et al. 2013; Stefansson et al. 2018) methods. The FE method has elaborate meshing capabilities and is mass conservative when utilizing the control volume finite element (CVFE) method (Forsyth 1990; Fung et al. 1992). Similarly, control volume finite-difference (CVFD), when the FV approach is applied to FD, can be used with flexible discretization (Ponting 1989; Heinemann et al. 1991) when combined with a multipoint flux approximation (MPFA) scheme (Edwards and Rogers 1998; Aavatsmark 2002). MPFA utilizes multiple neighboring cells to construct gradient terms, which allows more rigorous treatment of irregular cell geometries and directional anisotropy.

MODFLOW has evolved over many decades in an attempt to better represent the geometry and tensor orientation of complex flow fields. MODFLOW-2000 hydrogeologic-unit flow (HUF) and model-layer variable-direction horizontal anisotropy (LDVA) (Anderman et al. 2002) packages allow upscaling of heterogeneous layers and can solve for anisotropy in the horizontal plane. The DISU and GNC packages of MODFLOW-USG (Panday et al. 2013) allow for flexible and unstructured gridding, and corrections for discretization that does not comply with CVFD requirements. Most recently, MODFLOW 6 (Langevin et al. 2017) combined the flexible gridding of MODFLOW-USG and incorporated the XT3D capability which solves the groundwater flow equation using CVFD with a three-dimensional (3D) MPFA. The advances of MODFLOW 6 should therefore overcome many of the perceived limitations of MODFLOW codes when simulating the geometries and flow orientation induced by sedimentary structures (Hoaglund and Pollard 2003; Li et al. 2010; Gao et al. 2021). Yet, given its recent release in 2017, MODFLOW 6 and its XT3D capability has been applied in few research studies (Bennett et al. 2019; Goode and Senior 2020).

This study highlights the shortcomings of MODFLOW versions prior to MODFLOW 6 in the context of modeling flow through sedimentary structures and evaluates MODFLOW 6's improved capacity to address them. We highlight the limitations of older MODFLOW versions by turning our attention to structures which are geometrically complex or which have directional anisotropy, both of which are almost always present and control flow in sedimentary basins (Yager et al. 2009). We initially undertake benchmark simulations to assess traditional and contemporary discretization methods and solvers in MODFLOW, before applying our findings to a case study which compares modeled hydraulic heads and groundwater fluxes between MODFLOW 6 and prior versions. Finally, we discuss the significance of discretization methods and the use of MPFA for real world applications.

Benchmarks

Purpose

Groundwater flow is directed by sedimentary structures because of their boundaries of contrasting conductivity, as well as directional anisotropy. Therefore, groundwater models must preserve the geometric shape of structures, as well as the directional alignment of principal conductivity. The purpose of this section is to benchmark MODFLOW's past and current ability to estimate flow using different types of grids (1), along structure boundaries (2) and with a dipping conductivity tensor (3). These requirements may be distilled by benchmarking MODFLOW's ability to estimate flow through a dipping highly conductive anisotropic layer in a low conductivity domain.

Methodology

The individual impact of grid design, geological boundaries and anisotropic conductivity can all be tested using a simple model consisting of an idealized tilted channel (Figure 1). The idealized channel eliminates irregularities from real-life structures and allows comparison of numerically simulated hydraulic head and flow to an analytical solution. The benchmark model is in two-dimensional and can be considered as either plan or in transect, representing a sand channel or dipping sand layer, respectively. Both scenarios exhibit an identical analytical solution.

A head boundary function was imposed to induce a hydraulic gradient in the same orientation as the channel:

$$h(x, y) = i_u \cos\theta\, x + i_u \sin\theta\, y \qquad (1)$$

where $h(x, y)$ is the head at cell center coordinates at x and y (or z in transect), i_u is the hydraulic gradient parallel to the direction of the channel, and θ is the orientation of the channel from the x-axis.

Parameters used for the benchmark are presented in Table 1. Hydraulic conductivity of the structure is treated as isotropic for two analyses (Sections 2.3.1 and 2.3.2) and anisotropic for the last analysis (Section 2.3.3). A very low permeability domain (K_{domain}) surrounds the sand facies so flow is constrained to within the sand to allow an analytical solution for both flux and volumetric flow. This novel setup is particularly useful for the purpose of computational benchmarking, as it allows comparison with the analytical solution of the flow. The analytical flux (q_u) within the channel is equal to $K_{\max} \times i_u$, that is, 1 m/d in the direction of θ given our set of parameters.

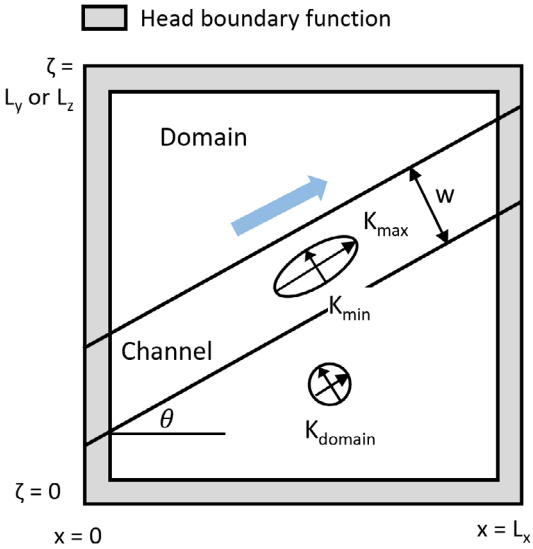

Figure 1. Model setup for the benchmarks for both plan ($\zeta = y$) and transect ($\zeta = z$) of a tilted sand channel in a low conductivity domain. The blue arrow represents the head gradient across the entire model, and flux within the channel.

Table 1
Parameters Utilized for Benchmark Simulations (Figure 1)

Parameter	Value
L_x	1000 m
L_y/L_z (plan)	1000 m/1 m
L_z/L_y (transect)	1000 m/1 m
w	200 m
K_{max}/K_{min}	1 m/d/1 m/d
K_{domain}	10^{-6} m/d
Theta (θ)	30°
Hydraulic gradient (i_u)	1 m/m
Analytical flux in channel (q_u)	1 m/d
Analytical flow through channel (Q_u)	200 m^3/d

Despite the hydraulic similarity of the plan and transect scenarios, the discretization options of MODFLOW are specific to each orientation (presented with results in Figure 3). Plan scenarios consider both rectilinear discretization and flexible triangular discretization, implemented so that they contain a similar number of cells. Flexible discretization allows cell edges to align with the channel boundary, generating realistic geometries with fewer cells, while hydraulic properties are assigned to rectilinear grid cells according to the proportion of cell area in the channel boundary. Flexible discretization was achieved using a triangle mesh generator (Shewchuk 1996) as inputs to the DISV package available in MODFLOW 6. Transect options are limited by MODFLOW's flat cell top and bottom requirement, meaning flexible grids in transect is not possible. In transect, we consider rectilinear as well as vertically offset discretization. Vertically offset represents hydraulic units as continuous layers where the depth and thickness of model layers are set to represent the geological layer. Rectilinear requires more cells than vertically offset, as well as preprocessing to assign hydraulic conductivities to cells which do not necessarily follow hydrogeologic layers (Anderson et al. 2015). Jupyter Notebooks for the benchmarks are included as Supporting Information.

Results

Capability to Model Flow Through Dipping Isotropic Layer

The benchmark compares numerical head and flux using three different grid construction methods: rectilinear (plan and transect), flexible triangular (plan) and vertically offset (transect). Here, we verify whether flow in dipping layers is robustly solved for all grid construction methods by measuring the flux value at the center of the channel far from the edges, where boundary effects are minimal, and comparing this to the analytical solution. Those results are visualized in Figure 2.

We can observe that the analytical flux, 1 m/d at 30°, is reproduced with the rectilinear grid (Figure 2a). It should be noted that MPFA essentially reduces to TPFA (Figure 2b) for isotropic rectilinear grids as this is already accurate (Provost et al. 2017). Without MPFA, the flexible grid produces perturbed heads and fluxes (Figure 2c) caused by the distorted grids and cell center connections which are not perpendicular to cell faces. However, this issue is resolved with MPFA (Figure 2d).

Vertically offset discretization produces a +15% error in flux magnitude, and more significantly a nearly horizontal head gradient and flux direction, rather than at 30° and aligned with the channel (Figure 2e). The flux direction error is not a problem of head boundary values given that the homogeneous case, that is when K_{domain} is equal to K_{channel}, produces the expected diagonal flow (Appendix S1). Preliminary analysis (Provost, A. and Langevin, C, personal communication, August 2022) suggests that the primary source of error is insufficient connectivity, and therefore insufficient hydraulic communication, between cells in adjacent grid layers in the channel. An interpolation scheme such as XT3D is unable to compensate for the error (Figure 2f) because the issue is largely one of connectivity, and not simply a matter of irregular geometry. The error in the flux magnitude and direction is particularly evident in the heterogeneous case of our benchmark due to the relatively large vertical offsets between cells and the hydraulic isolation of the channel from the rest of the model domain, which serves to suppress the vertical flows between grid layers that are necessary for an accurate solution within the channel. Further investigation is needed to verify this hypothesis and develop a practical approach to incorporating the appropriate grid connectivity into MODFLOW models with large vertical offsets between cells.

The outcome of this benchmark is that diagonal head gradients are well represented for rectilinear and flexible

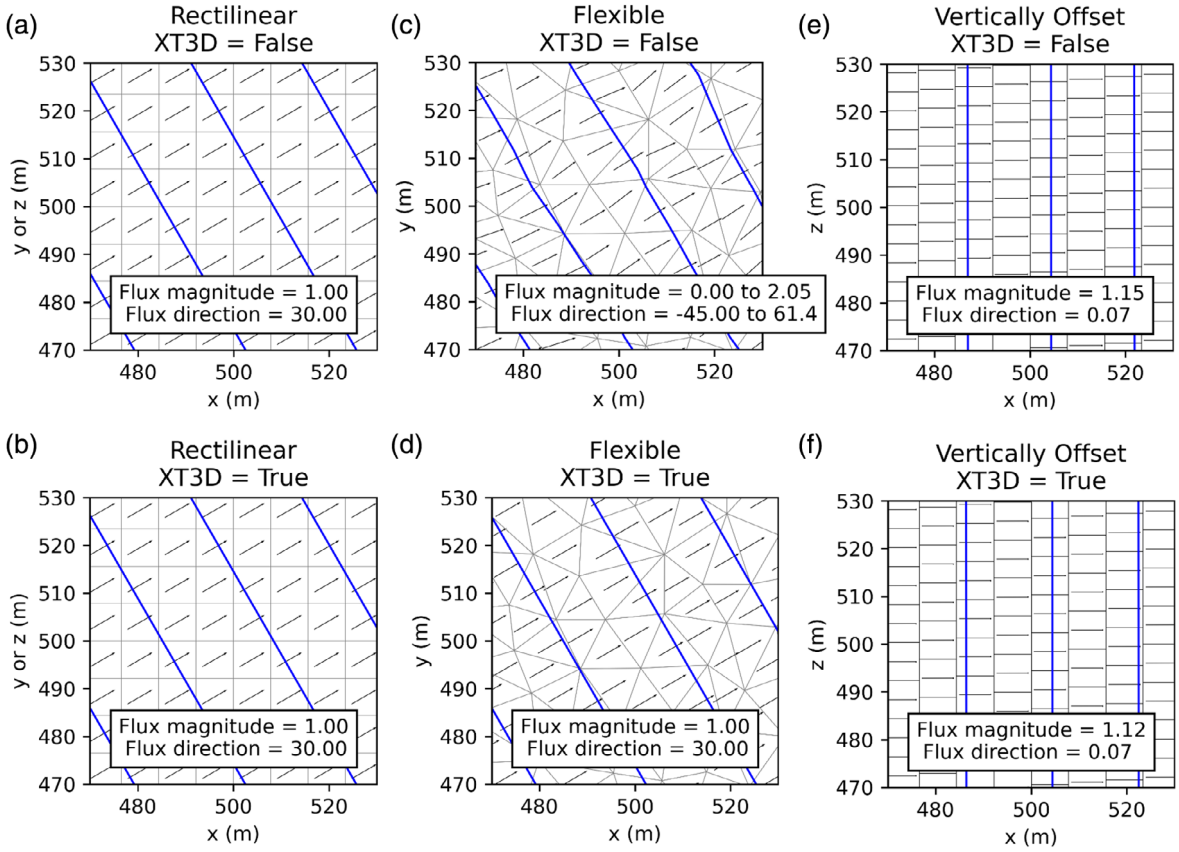

Figure 2. Discretization and simulated head contours and flux vectors for an isotropic zoomed-in domain within the middle of the channel. Rectilinear, flexible and vertically offset discretizations are explored, with the option of the XT3D option set to off (top row) and on (bottom row). The analytical head and flux solution is reached for scenarios a, b and d (i.e., 1 m/d at 30°).

grids, but vertically offset grids are not yet suitable for steeply dipping heterogeneous layers where a diagonal head gradient is imposed.

Capability to Model Flow Along Dipping Layer Boundary

Rectilinear and vertically offset discretizations, which are the only options for MODFLOW versions previous to MODFLOW 6, result in the rasterization of structure boundaries (Figure 3c). We investigate errors due to this approximation by drawing our attention to fluxes at the channel boundary, expecting flow to be parallel with the boundary. Therefore, we examine fluxes at the channel boundary for all discretization scenarios (Figure 3a through 3c), as well as translating this to implications for total flow by integrating fluxes (Figure 3d). We also investigate the effect of resolution by increasing the number of cells used in the simulation.

As expected from its original purpose, flexible discretization has no boundary effect, with fluxes at the boundary staying consistent (Figure 3a), and the volumetric flow conforming to the analytical solution even for coarse resolutions (green line in Figure 3d). Despite its visually rasterized representation, the vertically offset grid does not suffer from boundary effects (Figure 3b), an artifact of inappropriate hydraulic connectivity. However, the overestimated flux as previously identified causes the volumetric flow through the channel to be equally overestimated and does not improve with resolution (blue line in Figure 3d). The rectilinear grid, however, produces irregular flux magnitudes and directions for cells along the channel boundary (Figure 3c), which we coin as the "staircase effect" given the way that flow must make its way along the boundary in a convoluted way. The retardation of fluxes at the boundary subsequently reduces the volumetric flow through the channel, which improves with resolution due to a smaller percentage of channel cells being located along the boundary (orange line in Figure 3d). A grid convergence study was done for the rectilinear scenario showing that convergence of volumetric flow to the analytical follows a power law of exponent −1, consistently found with the staircase effect (Kereyu and Gofe 2016). Therefore, to restrict the error of the flow through a 30° tilting channel to within 5% and 10%, 20 and 10 cells per channel width, respectively, are necessary. While the rectilinear staircase error is resolution-dependent, the vertically offset error is not. Therefore, if rectilinear discretization is not able to adequately refine dipping structures due to computational limitations, then vertically offset would be the less erroneous option. The transition point of the required rectilinear resolution to better vertically offset for the benchmark is 5 cells per channel width, the point

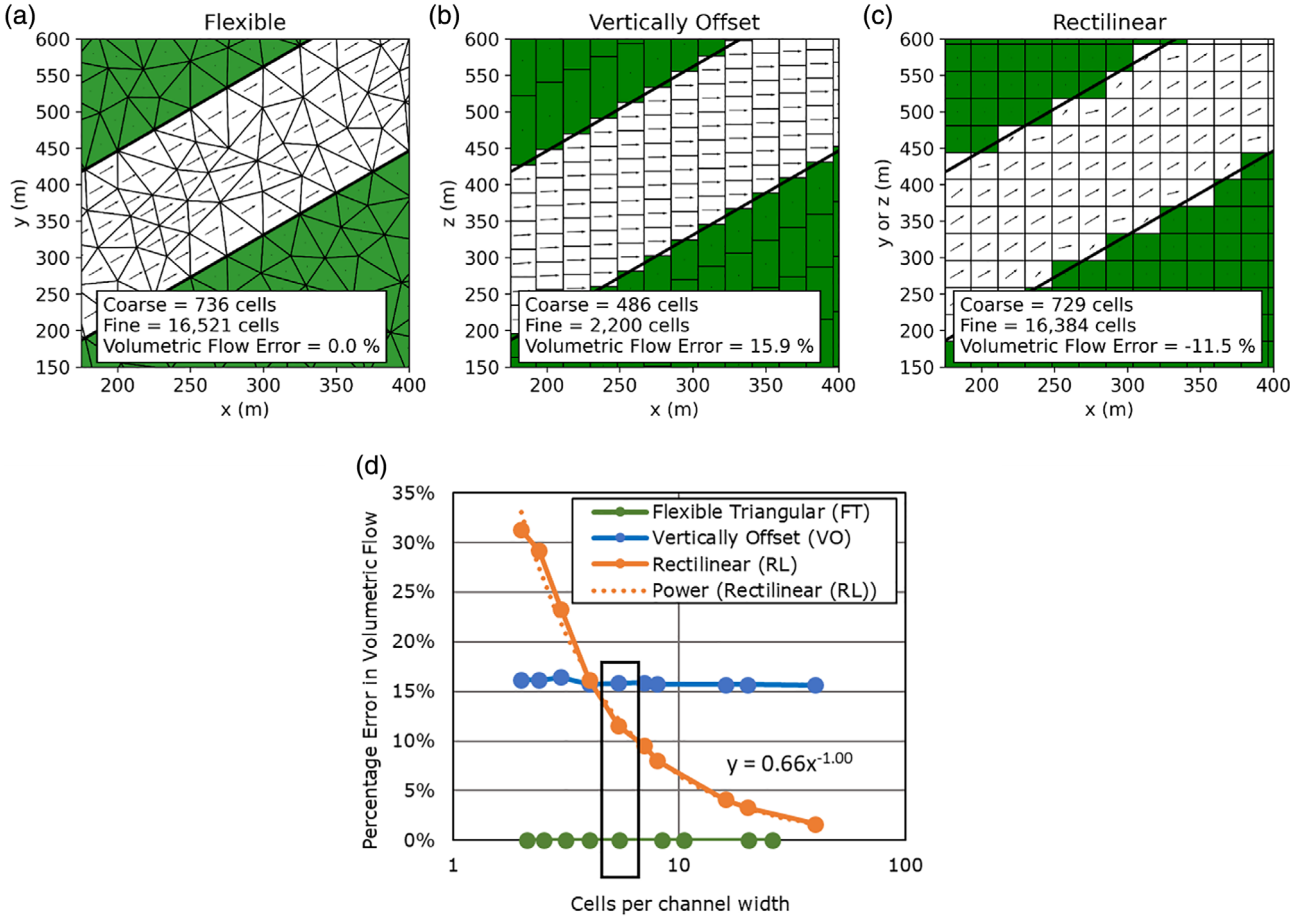

Figure 3. Discretization schemes deployed for the benchmarks (a to c), with the fine discretization used for the benchmarks but the coarse discretization represented here for clear visualization. Volumetric flow rate error compared to the analytical solution with changing resolution (d). For the flexible grid, cells per channel width is based on an equivalent number of cells for a structured grid. The black rectangle highlights the scenarios visually represented in a to c. The intersection between the orange and blue line represents the cross-over point where rectilinear has less error than vertically offset grids.

where the orange and blue line crosses in Figure 3d. The transition point would depend on the angle of the structure.

This benchmark highlights one of the benefits of flexible gridding, which represents accurate fluxes and flows even at a coarse scale, whereas rectilinear grids require more refinement due to rasterization of boundaries.

Capability to Model Flow Through Dipping Anisotropic Layer

Simulation of flow through dipping anisotropic layers requires every component of the hydraulic conductivity tensor (Aavatsmark et al. 1998), which MODFLOW codes prior to MODFLOW 6 were not designed to handle. Instead, MODFLOW 6's MPFA scheme, activated using the XT3D option, uses a larger stencil and weighted interpolation to allow for the consideration of the full tensor. Here we benchmark MODFLOW 6 and prior MODFLOW versions capability for modeling flow in a dipping anisotropic channel. Given that anisotropy is typically considered between the horizontal and vertical direction, and that intra-cell fluxes computed on vertically offset grids are still subject to significant loss of accuracy in steeply dipping channels, we focus on the transect scenario, with the rectilinear grid. The previous simulations have used an isotropic conductivity tensor, and now we replace this with a varying anisotropic tensor in the direction of the channel (30°).

We find that the flux magnitude when using TPFA is extremely diminished, up to 0.28% of the analytical flux for 1000:1, while MPFA matched the analytical flux to 99.97% (Table 2).

We extend this particular benchmark to include multiple dips and anisotropy ratios for TPFA and MPFA, and then recover the effective conductivity ellipses based on outputted fluxes. Please refer to Appendix S2 for methodology and Jupyter Notebook S3. The effective conductivity ellipses (Figure 4a) show that MPFA matches the input conductivity, whereas the TPFA ellipses are diminished, at its worst at 45°. The TPFA method essentially truncates the inputted conductivity tensor by setting the off-diagonal components of the K tensor to zero, and uses the x and y components of the ellipse radius at angle theta for the diagonal components (Langevin et al. 2017). As we increase the anisotropy ratio, we increase the magnitude of the error (Figure 4b). Effective conductivity drops steeply to only a fraction of its input

Table 2
Computed Fluxes, q_{mag} (m/d), Flux Direction, q_{theta} (°) and Model Run Time (s) for the Benchmark in Figure 1 with an Anisotropic Conductivity Tensor

	Analytical		MPFA			TPFA		
K_{max}:K_{min}	q_{mag}	q_{theta}	q_{mag}	q_{theta}	Run Time	q_{mag}	q_{theta}	Run Time
1:1	1	30	1.003	30.00	0.409	1.003	30.00	0.394
10:1	10	30	10.008	29.99	1.716	2.359	29.93	0.249
100:1	100	30	100.006	29.99	0.539	2.735	29.92	0.282
1000:1	1000	30	999.697	29.99	0.577	2.780	29.91	0.247

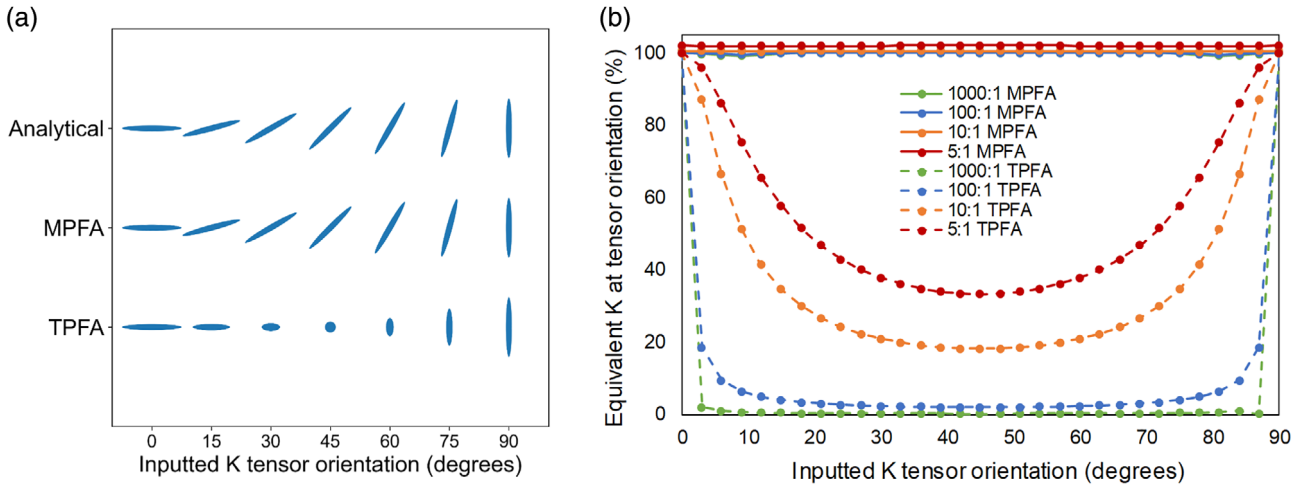

Figure 4. (a) Effective conductivity ellipsoids for two-point flux approximation (TPFA) and multipoint flux approximation (MPFA, implemented using the XT3D option) compared to the analytical for K_{max}:K_{min} of 10:1. (b) Effective conductivity as a percentage of the analytical value for various tensor angles, anisotropy ratios and numerical scheme (TPFA vs. MPFA).

value for high anisotropy, for example a 3° dip with 1000:1 anisotropy produces an equivalent conductivity of only 27% of its actual value.

This benchmark highlights that MODFLOW versions prior to MODFLOW 6 are far from robust for modeling flow through highly anisotropic and dipping layers, and that MODFLOW 6's XT3D capability must be used. However, it should be noted that at high anisotropy ratios, MPFA can be susceptible to spatial oscillations in the solution, and users of the option should critically evaluate results to check there are no sources or sinks present that are unrealistic (Provost et al. 2017). An example that focuses on correcting this issue, in this case for the dispersion tensor rather than the conductivity tensor, is for MT3DMS, the transport package used with MODFLOW (Yan and Valocchi 2020).

Case Study

Here, we present a case study where we apply our recommendations for modeling structure with MODFLOW on a real basin with an existing groundwater model. The site exhibits multiple superimposing aspects associated with sedimentary structures, including irregular shaped structures in plan and dipping anisotropic layers, as well as sharp changes in flow direction. The purpose is to showcase the resulting differences in modeled flow patterns between using traditional and contemporary MODFLOW discretization methods, and once again assert the significance of MODFLOW 6's new packages.

Perth Regional Aquifer Modeling System

The Perth Basin contains vast amounts of groundwater which supplies approximately 70% of water supply for Perth, Western Australia (De Silva et al. 2013). It is a sedimentary rift basin comprising around 12 km of sediments and hosting multiple major aquifers (Davidson 1995). Of note is the superficial unconfined aquifer which overlies the Leederville and Yarragadee confined aquifer systems. These three systems are separated by two major confining units, the Kardinya and South Perth Shales, respectively, which are often thick and extensive, but not conformable at all locations. The aquifers are bounded to the east at the Darling Fault by Archean crystalline rocks, and groundwater flows predominantly west toward the ocean, although there is some mounding in recharge zones which influences local flow patterns. Recharge to the superficial aquifer is primarily through rainfall, with leakage replenishing the underlying confined aquifers where aquitards are absent. The Swan River is a major drainage

pathway running North-East to South-West (see Supporting Information, Figure S1 for a locality plan).

The Perth Regional Aquifer Modeling System (PRAMS 3.5.2) is a coupled recharge and groundwater model, initially built in the early 2000 s for the purpose of managing the complex groundwater needs of Perth (De Silva et al. 2013; Siade et al. 2017). PRAMS covers a surface area of 9100 km^2 and utilizes a modified version of MODFLOW-2000 that incorporates a landscape model known as the Vertical Flux Manager (Silberstein et al. 2009), which employs the WAVES software for simulating flow though the unsaturated zone and ultimately groundwater recharge (Dawes et al. 2012). PRAMS 3.5.2 is discretized into 500 × 500 m cells in plan and consists of 454 rows and 214 columns with approximately 600,000 active cells and runs for 13 years with monthly time steps resulting in a CPU runtime of approximately 2 to 3 h on most common desktop computers (Siade et al. 2020). Thirteen vertically offset layers represent the main sedimentary units, which are mostly extensive with some pinch-outs. The Kings Park formation is an intrusive unit which incises multiple layers and is represented as a change in conductivity in the incised layer. The structure of the basin results in dipping of up to 15°, such as the South Perth Shale around the Joondalup area.

Methodology

Our aim is to compare the current PRAMS model which uses MODFLOW-2000, with its MODFLOW 6 counterpart to investigate the impact of available discretization options and numerical schemes on modeled flow patterns.

We extract two submodels from PRAMS, one in plan and the other in transect. In plan, the submodel is centered on the intrusive Kings Park formation as it represents irregular geometry and an ideal candidate to apply flexible gridding. The transect submodel runs 11.5 km in a north-south direction across a major dip. The submodels are created by extracting arrays of horizontal and vertical conductivity from PRAMS, as well as head values and recharge for a typical snapshot in time. The models are run in steady-state to observe how model discretization affects long-term flow patterns. More details on methodology specific to each orientation are discussed below.

Plan Submodel

The plan submodel was created from PRAMS Layer 7 which represents the Wanneroo Member of the Leederville aquifer, which is incised from the west by the Kings Park formation. The Wanneroo Member has a relatively high horizontal conductivity (estimated at 6 m/d), with the Kings Park Formation being less conductive at 1 m/d.

Three discretization scenarios in plan were created (Figure 5 and Table 3): (1) the original PRAMS discretization; (2) flexible triangular, as recommended from the benchmarks; and (3) fine rectilinear, which was shown from our benchmarks to accurately represent complex flow and corresponds to our reference case. The flexible gridding scenario can be locally refined and coarsened in different ways, however here we aim to have a similar number of cells as PRAMS. Heads along all four boundaries were extracted from the PRAMS submodel and marked as constant heads, and linearly interpolated for cell centers along the flexible and rectilinear model boundaries.

Fluxes for the flexible grid are streamlined along the formation boundary and better represent fine rectilinear despite using approximately the same number of cells as PRAMS (Figure 5). Rasterization of the boundaries of the Kings Park Formation using PRAMS causes the formation to artificially narrow resulting in a misleading flowpath (point A) and induces flow that is not streamlined around the formation edge due to the staircase effect (point B). Instead, the flexible grid represents the flow regime around the formation edge and allows for more refinement flexibility, which is key for maximizing numerical accuracy in critical areas such as along model boundaries, geological boundaries and pumping zones.

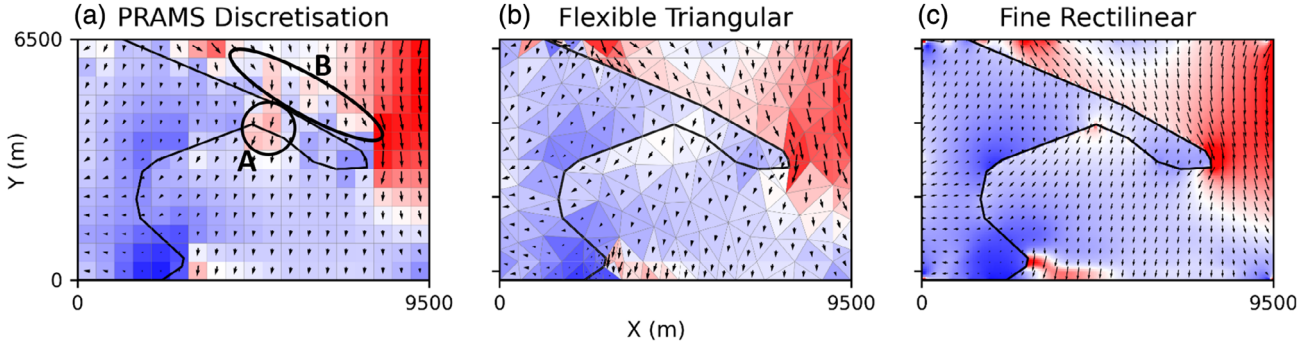

Figure 5. Three discretization scenarios of the Kings Park Formation are compared: (a) PRAMS discretization (b) flexible triangular and (c) fine rectilinear. Thick black lines represent the boundary of the Kings Park Formation and cells are colored according to flux magnitude, with red being high flux and blue being low. PRAMS discretization produces a short circuit in flowpath at A and irregular flow along the structure boundary at B.

Table 3
Case Study Scenarios Considered

Orientation	Discretization	Resolution
Plan Focussing on intrusive and irregular Kings Park Formation	PRAMS discretization	288 cells (12 rows, 24 columns)
	Flexible triangular	322 cells
	Fine rectilinear	28,800 cells (20 rows, 240 columns)
Transect Focussing on dipping anisotropic layers	PRAMS discretization	299 cells (13 layers, 60 columns)
	Coarse rectilinear	15,000 cells (150 layers, 100 columns)
	Fine rectilinear	23,400 cells (390 layers, 260 columns)

Transect Submodel

The transect submodel investigates differences in modeled head and flux for dipping anisotropic layers. The transect submodel contains a maximum dip of 7° and maximum anisotropy ratio of 30,000:1 based on the PRAMS calibration. Three scenarios were considered in transect: (1) original PRAMS discretization which uses a vertically offset grid with TPFA; (2) coarse rectilinear discretization with rotated conductivity tensors and MPFA, as recommended from the benchmarks; and (3) fine rectilinear discretization with rotated conductivity tensors and MPFA as our reference case as it accurately represents flow (Table 3). PRAMS contains 13 vertically offset layers, each layer representing a significant geological sequence in the Perth Basin. Hydraulic properties are overlayed onto the coarse and fine rectilinear models, with careful refinement so that the true thickness of geological layers is well represented and not over rasterized. Computation of the 9000 cells in the coarse rectilinear model is expensive when compared to the 299 cells used in PRAMS. However, this number could be reduced by refining in the Z direction as needed, instead of applying a blanket Z direction discretization step.

Conductivity tensor angles used in the rectilinear scenarios are calculated using the dip of the bottom of each geological formation, although this could have been done instead for the center of the layer, depending on the interpreted bedding angle. Generally however, the formation bottom best represents depositional angle given that formation bottoms are generally conformable. The left and right boundaries are assigned constant heads, the bottom a no-flow condition and recharge is added along the top. Boundary heads are linearly interpolated for the rectilinear scenarios. Modeled fluxes for each method are compared by integrating fluxes vertically across the transect for cells pertaining to each of the 13 original layers.

There are striking differences in flux results between PRAMS and coarse rectilinear, particularly around sloping units (Figure 6). First, we can observe, by comparing transects showing vertical flux (Figure 6a and 6b), that the rectilinear scenario introduces a wider range in vertical fluxes within the Wanneroo and Yarragadee aquifers, and that flow direction is influenced by the shape of the aquitard. The PRAMS model significantly under estimates vertical fluxes, with almost no vertical flux modeled in the Wanneroo layer, yet greater than 0.00015 m/d for some sections in the rectilinear scenario (Figure 6c). Second, horizontal flux in the primary aquifer of interest, the Wanneroo Member, is approximately 10 to 20% more in PRAMS than the rectilinear scenario (Figure 6d). As in our benchmarks, these results show that using TPFA on vertically offset grids can significantly underestimate vertical fluxes. This may result in contaminants being modeled as moving primarily horizontally, which may not be accurate for sloping layers.

Conclusion

This paper revisits MODFLOW's capability to model flow through sedimentary structures, which are typically irregular in geometry with anisotropic conductivity. Benchmark simulations have highlighted the limitations of MODFLOW 2005 and prior. The rasterization of hydraulic properties onto a structured grid causes a "staircase error" whereby modeled flow is retarded along interfaces between sedimentary structures where there is a sharp change in conductivity. We showed that the flow through a 30° tilted sand channel is underestimated by 8% due to the staircase error. More important is the gross under-estimation of flow through anisotropic dipping layers, associated with folded or tilted sedimentary structures, due to significant truncation of the conductivity tensor in the absence of an MPFA scheme. When MODFLOW-2005 is used to model flow through the same 30° tilted sand channel, flux within the channel is reduced to only 24%, 3%, and 0.3% of its actual value for anisotropy ratios of 10:1, 100:1, and 1000:1, respectively. However, we show that MODFLOW 6 has overcome some of these issues by including flexible discretization (DISV package) and an MPFA scheme (XT3D option). This has given MODFLOW similar capability as existing CVFE codes, such as SUTRA (Provost and Voss 2019), allowing robust modeling of flow through dipping anisotropic layers.

Persisting issues however include the pervading assumption that cells have flat tops and bottoms in transect, which produces the staircase error as well as

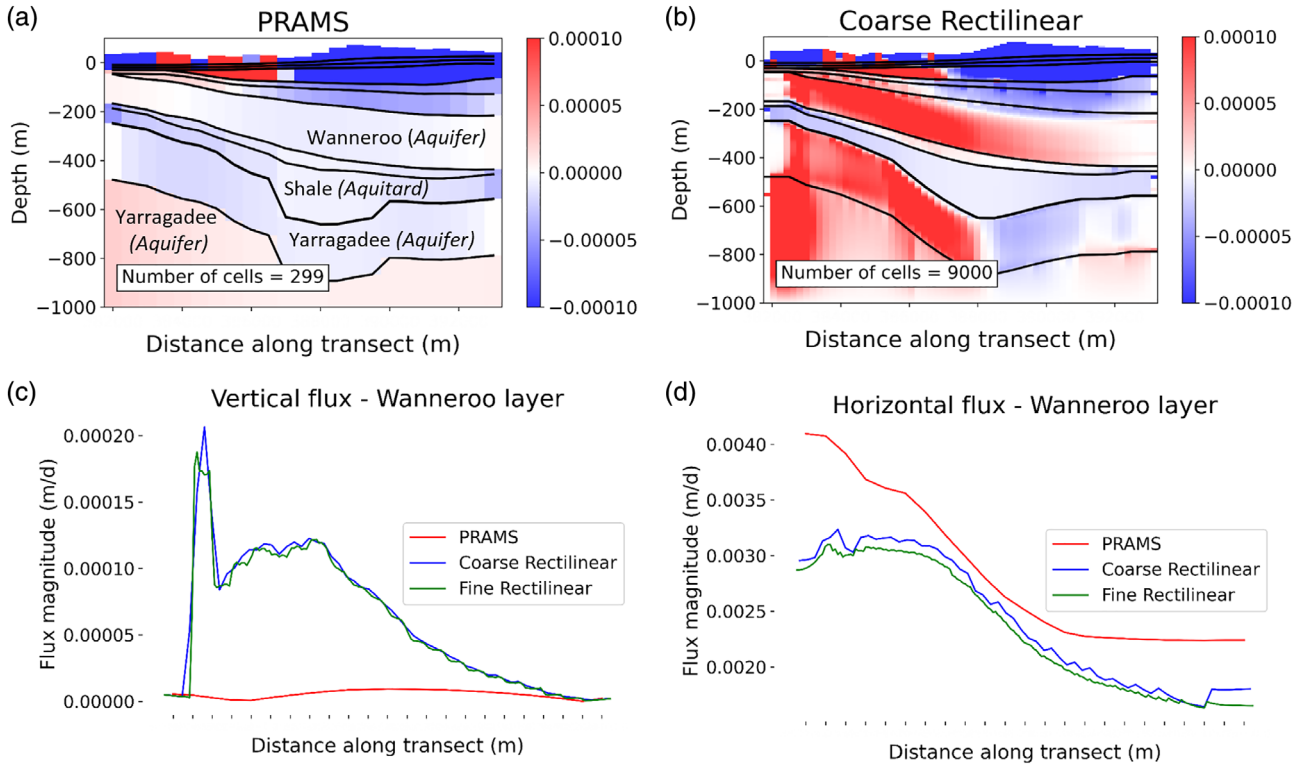

Figure 6. Vertical flux magnitudes using (a) PRAMS discretization, (b) coarse rectilinear, (c) and (d) vertical and horizontal fluxes, respectively, for the Wanneroo layer, the primary aquifer of interest. Blue represents downward flux and red represents upward flux.

requiring a large number of cells to adequately represent thin dipping layers using a regular grid. We show that vertically offset grids, while a numerically efficient way to represent gently dipping layers, can still be subject to significant loss of accuracy in head and flow estimates when the dip is steep, especially if the dipping layer is much more conductive than the surrounding material. We hypothesize that vertically offset grids to not provide sufficient connectivity between adjacent model layers to accurately simulate the steeply dipping, highly heterogeneous case.

The main recommendations from this research are that (1) vertically offset grids are further investigated as to their source of error, and that appropriate grid connectivity be incorporated in MODFLOW models with large vertical offsets between cells, (2) modelers of significantly dipping and anisotropic layers should be prepared to employ an expensive but necessary approach of overlaying properties onto a regular grid in transect and applying the XT3D option, or risk grossly underestimating groundwater flow magnitude; (3) given the increased computation required for MPFA solutions (refer Table 2), further research should focus next on automated refining and upscaling procedures, such as that suggested by Sbai (2020), and (4) FV models with unstructured discretization in 3D, such as the use of tetrahedron cells, would be a logical direction forward to truly represent the geometry and flow pathways generated by sedimentary structures.

Acknowledgment

This study was financially supported by the Australian Research Council, Department of Water and Environmental Regulation of Western Australia, Water Corporation of Western Australia and Rio Tinto Iron Ore through Grant Number LP180101153. We thank the two anonymous reviewers and Alden Provost for their comments which strengthened the manuscript. We also thank Alden Provost and Christian Langevin for discussions on vertically offset grids. Open access publishing facilitated by The University of Western Australia, as part of the Wiley - The University of Western Australia agreement via the Council of Australian University Librarians.

Authors' Note

The authors do not have any conflicts of interest or financial disclosures to report.

Supporting Information

Additional supporting information may be found online in the Supporting Information section at the end of the article. Supporting Information is generally *not* peer reviewed.

Appendix S1. Comparison results for homogeneous and heterogeneous scenarios.

Appendix S2. Methodology for extracting effective conductivity ellipses.

Figure S1. Locality plan for case study.
Jupyter Notebook S1. Plan benchmark.
Jupyter Notebook S2. Transect benchmark.
Jupyter Notebook S3. For anisotropy study.

References

Aavatsmark, I. 2002. An introduction to multipoint flux approximations for quadrilateral grids. *Computational Geosciences* 6, no. 3–4: 405–432.

Aavatsmark, I., T. Barkve, O. Boe, and T. Mannseth. 1998. Discretization on unstructured grids for inhomogeneous, anisotropic media. Part II: Discussion and numerical results. *Society for Industrial and Applied Mathematics* 19, no. 5: 1717–1736.

Anderman, E.R., K.L. Kipp, M.C. Hill, J. Valstar, and R. M. Neupauer. 2002. MODFLOW-2000, the U.S. Geological Survey modular ground-water model—Documentation of the model-layer variable-direction horizontal anisotropy (LVDA) capability of the hydrogeologic-unit flow (HUF) package. U.S. Geological Survey Open-File Report 02-409.

Anderson, M.P., W.W. Woessner, and R.J. Hunt. 2015. *Applied Groundwater Modeling: Simulation of Flow and Advective Transport*. Elsevier Science & Technology. https://www.sciencedirect.com/book/9780120581030/applied-groundwater-modeling

Bennett, J.P., C.P. Haslauer, M. Ross, and O. Cirpka. 2019. An open, object-based framework for generating anisotropy in sedimentary subsurface models. *Groundwater* 57, no. 3: 420–429.

Borghi, A., P. Renard, and G. Courrioux. 2015. Generation of 3D spatially variable anisotropy for groundwater flow simulations. *Groundwater* 53, no. 6: 955–958.

Catuneanu, O. 2006. *Principles of Sequence Stratigraphy*. Boston: Elsevier Science & Technology.

Davidson, W.A. 1995. Hydrogeology and groundwater resources of the Perth region, Western Australia. *Western Australia Geological Survey, Bulletin* 142: 257.

Dawes, W., R. Ali, S. Varma, I. Emelyanova, G. Hodgson, and D. McFarlane. 2012. Modelling the effects of climate and land cover change on groundwater recharge in south-West Western Australia. *Hydrology and Earth System Sciences* 16, no. 8: 2709–2722.

De Silva, J., P. Wallace-Bell, C. Yesertener, and S. Ryan. 2013. Perth regional aquifer modelling system (PRAMS) v3.5—Conceptual model. Department of Water, Western Australia, Hydrogeological Record Series Report No. HR334.

Edwards, M.G., and C.F. Rogers. 1998. Finite volume discretization with imposed flux continuity for the general tensor pressure equation. *Computational Geosciences* 2, no. 4: 259–290.

Forsyth, P.A. 1990. Control-volume, finite-element method for local mesh refinement in thermal reservoir simulation. *SPE Reservoir Engineering (Society of Petroleum Engineers)* 5, no. 4: 561–566.

Fossen, H. 2016. *Structural Geology*, 2nd ed. United Kingdom: Cambridge University Press.

Fries, T.P., M. Fücker, and A. Kauerauf. 2014. The finite element method with continuity constraints for stair-step grids in geoscience. *Computational Geosciences* 18, no. 5: 831–850.

Fung, L.S., A.D. Hiebert, and L.X. Nghlem. 1992. Reservoir simulation with a control volume finite element method. *SPE Reservoir Engineering* 1992, no. 8: 349–357.

Gao, Y., E. Du, S. Yi, Y. Han, and C. Zheng. 2021. An improved numerical model for groundwater flow simulation with MPFA method on arbitrary polygon grids. *Journal of Hydrology* 606: 127399.

Goode, D.J., and L.A. Senior. 2020. Groundwater withdrawals and regional flow paths at and near Willow Grove and Warminster, Pennsylvania—Data Compilation and preliminary simulations for conditions in 1999, 2010, 2013, 2016, and 2017. U.S. Geological Survey Open-File Report 2019–1137.

Harbaugh, A. W. 2005. MODFLOW-2005, The U. S. Geological Survey modular ground-water model—The ground-water flow process. U.S. Geological Survey Techniques and Methods 6-A16.

Heinemann, Z.E., C.W. Brand, M. Munka, and Y.M. Chen. 1991. Modeling reservoir geometry with irregular grids. *SPE Reservoir Engineering (Society of Petroleum Engineers)* 6, no. 2: 225–232.

Hoaglund, J.R., and D. Pollard. 2003. Dip and anistropy effects on flow using a vertically skewed model grid. *Groundwater* 41, no. 6: 841–846.

Kereyu, D., and G. Gofe. 2016. Convergence rates of finite difference schemes for the diffusion equation with Neumann boundary conditions. *American Journal of Computational and Applied Mathematics* 6, no. 2: 92–102.

Koltermann, C.E., and S.M. Gorelick. 1996. Heterogeneity in sedimentary deposits: A review of structure-imitating, process-imitating, and descriptive approaches. *Water Resources Research* 32, no. 9: 2617–2658.

Kumar, C.P. 2019. An overview of commonly used groundwater modelling software. *International Journal of Advanced Research in Science, Engineering and Technology* 6, no. 1: 7854–7865.

Langevin, C.D., J.D. Hughes, E.R. Banta, R.G. Niswonger, S. Panday, and A.M. Provost. 2017. Documentation for the MODFLOW 6 groundwater flow model. U.S. Geological Survey Techniques and Methods 6-A55.

Li, L., H. Zhou, and J.J. Gómez-Hernández. 2010. Steady-state saturated groundwater flow modeling with full tensor conductivities using finite differences. *Computers and Geosciences* 36, no. 10: 1211–1223.

Michael, H.A., and C.I. Voss. 2009. Estimation of regional-scale groundwater flow properties in the Bengal Basin of India and Bangladesh. *Hydrogeology Journal* 17, no. 6: 1329–1346.

Oriani, F., and P. Renard. 2014. Binary upscaling on complex heterogeneities: The role of geometry and connectivity. *Advances in Water Resources* 64: 47–61.

Panday, S., C.D. Langevin, R.G. Niswonger, M. Ibaraki, and J.D. Hughes. 2013. MODFLOW–USG version 1: An unstructured grid version of MODFLOW for simulating groundwater flow and tightly coupled processes using a control volume finite-difference formulation. U.S. Geological Survey Techniques and Methods 6-A45.

Ponting, D.K. 1989. Corner point geometry in reservoir simulation. In *ECMOR I—1st European Conference on the Mathematics of Oil Recovery*. European Association of Geoscientists and Engineers: 45–65.

Provost, A.M, and C.I. Voss. 2019. SUTRA, a Model for saturated-unsaturated, variable-density groundwater flow with solute or energy transport—Documentation of generalized boundary conditions, a modified implementation of specified pressures and concentrations or temperatures, and the lake capability. U.S. Geological Survey, Techniques and Methods 6-A52.

Provost, A.M., C.D. Langevin, and J.D. Hughes. 2017. Documentation for the 'XT3D' option in the Node Property Flow (NPF) package of MODFLOW 6. U.S. Geological Survey, Techniques and Methods 6-A56: 50.

Renard, P., and D. Allard. 2013. Connectivity metrics for subsurface flow and transport. *Advances in Water Resources* 51: 168–196.

Rühaak, W., V. Rath, A. Wolf, and C. Clauser. 2008. 3D finite volume groundwater and heat transport modeling with

non-orthogonal grids, using a coordinate transformation method. *Advances in Water Resources* 31, no. 3: 513–524.

Sbai, M.A. 2020. Unstructured gridding for MODFLOW from prior groundwater flow models: A new paradigm. *Groundwater* 58, no. 5: 685–691.

Shewchuk, J.R. 1996. Triangle: Engineering a 2D quality mesh generator and Delaunay triangulator. In *Applied Computational Geometry Towards Geometric Engineering*. *WACG 1996*. *Lecture Notes in Computer Science*, Vol. 1148, ed. M.C. Lin, and D. Manocha. Berlin, Heidelberg: Springer.

Siade, A., T. Cui, R.N. Karelse, and C. Hampton. 2020. Reduced-dimensional Gaussian process machine learning for groundwater allocation planning using swarm theory. *Water Resources Research* 56, no. 3: 1–21.

Siade, A., J. Hall, and R.N. Karelse. 2017. A practical, robust methodology for acquiring new observation data using computationally expensive groundwater models. *Water Resources Research* 53, no. 11: 9860–9882.

Silberstein, R., A. Barr, G. Hodgson, D. Pollock, R. Salama, and T. Hatton. 2009. *A Vertical Flux Model for the Perth Groundwater Region*. Perth, Western Australia: Department of Water Hydrogeological record series no. HG33.

Stefansson, I., I. Berre, and E. Keilegavlen. 2018. Finite-volume discretisations for flow in fractured porous media. *Transport in Porous Media* 124, no. 2: 439–462.

Yager, R.M., C.I. Voss, and S. Southworth. 2009. Comparison of alternative representations of hydraulic-conductivity anisotropy in folded fractured-sedimentary rock: Modeling groundwater flow in the Shenandoah Valley (USA). *Hydrogeology Journal* 17, no. 5: 1111–1131.

Yan, S., and A.J. Valocchi. 2020. Flux-corrected transport with MT3DMS for positive solution of transport with full-tensor dispersion. *Groundwater* 58, no. 3: 338–348.